ELSEVIER

International Journal of Pharmaceutics 238 (2002) 229–239

international journal of pharmaceutics

www.elsevier.com/locate/ijpharm

Coating of cationized protein on engineered nanoparticles results in enhanced immune responses

Zhengrong Cui, Russell J. Mumper *

Division of Pharmaceutical Sciences, College of Pharmacy, University of Kentucky, Lexington, KY 40536-0082, USA

Received 29 October 2001; received in revised form 25 January 2002; accepted 20 February 2002

Abstract

A significant emphasis has been placed on the development of improved adjuvants and delivery systems to improve both antibody production and cell-mediated immunity. The overall goal of this project was to cationize a model protein antigen, β-galactosidase (nGal), coat the cationized Gal (cGal) on the surface of novel anionic nanoparticles engineered from microemulsion precursors, and assess the immune response of this system after subcutaneous injection to mice. Gal was chemically cationized as evidenced by gel electrophoresis. The cGal was coated on anionic nanoparticles (78 ± 11 nm) engineered from oil-in-water microemulsion precursors to produce cGal-coated nanoparticles. The immune response to nGal with 'Alum', cGal alone, and cGal-coated nanoparticles were assessed after subcutaneous injection to Balb/c mice. cGal alone elicited similar antibody titer to nGal with 'Alum'. However, cGal-coated nanoparticles elicited the strongest and most reproducible antibody titer. cGal alone produced very high levels of Th1 cytokines, but low levels of Th2 cytokines. In contrast, cGal-coated nanoparticles significantly enhanced both the Th1 and Th2 cytokines. The results demonstrated the utility of antigen-coated nanoparticles to enhance both the humoral and Th1-type immune responses, in parallel.

Keywords: β-Galactosidase; Microemulsion; Immunization; T-helper cell; Cytokine; Sodium dodecyl sulfate

1. Introduction

Vaccines are generally divided into two categories, live and non-live vaccines (Plotkin et al., 1988). Although the non-live vaccines, especially the recombinant protein subunit vaccines, have some advantages over traditional live vaccines, a general problem associated with the protein subunit vaccines is that they are poorly immunogenic when administrated alone without adjuvants (Gupta et al., 1995). However, despite intensive searches for newer and better adjuvants, 'Alum' still remains as the only approved adjuvant for human use. Although the 'Alum' has been used in vaccines for many years, it is generally regarded as a weak adjuvant for antibody induction and most importantly, a poor adjuvant for cell-mediated immunity (Gupta et al., 1993).

In recent years, a significant emphasis has been placed on the development of improved adjuvants

* Corresponding author. Tel.: +1-859-257-2300x258; fax: +1-859-323-5985.

E-mail address: rjmump2@pop.uky.edu (R.J. Mumper).

0378-5173/02/$ - see front matter
PII: S0378-5173(02)00079-0

and delivery systems to improve antibody production and cell-mediated immunity. New adjuvants and delivery systems must be potent, safe, economical, and compatible with the new generation of vaccines, including protein subunit vaccines. These new agents can generally be divided into two groups, novel immunostimulatory molecules and particles. For example, QS21, an isolated pure fraction of Quil A saponin, has been shown to be a potent adjuvant for cytotoxic T-lymphocyte (CTL) induction, inducing T-helper cell Type 1 (Th1) cytokines Interleukin-2 (IL-2) and Interferon-γ (IFN-γ) secretion (Kensil, 1996). QS21 may be a potential adjuvant for vaccines against pathogens that require a potent CTL response if it can be demonstrated in wide-spread human clinical trials to meet the criteria as defined above. Examples of particulate adjuvants include emulsions such as Freund's complete adjuvant, Incomplete Freund's adjuvant (Sheikh et al., 2000), molecules and complexes such as MF59 (Singh et al., 1999), immunostimulatory complexes (ISCOMS) (Morein et al., 1990), and colloidal carriers such as liposomes (Alving, 1991) and other micro- and nanoparticles (O'Hagan et al., 1991; Singh et al., 2000; Kazzaz et al., 2000; Cui and Mumper 2001a,b, 2002a,b; Muller et al., 2000; Moser et al., 1997; Ocampo et al., 2000). It is not surprising that such particulates act as adjuvants since these synthetic particles have much in common with natural particulate pathogens such as viruses and bacteria. Fortunately, in most cases, the human immune system has evolved and can adapt to combat these natural particulate pathogens via phagocytosis by macrophages and other antigen-presenting cells. The use of micro- and nanoparticles as adjuvants has been demonstrated by a number of groups over the last two decades (O'Hagan, 1997). For example, protein antigens have been incorporated into the biodegradable microspheres comprised of polylactic-co-glycolic acid (PLGA) which have been used to induce potent humoral and cytotoxic T-lymphocyte (CTL) immune responses (O'Hagan, 1997). Further, it has been confirmed that simple adsorption of either DNA vaccines or protein subunit vaccines on the surface of preformed micro- and nanoparticles can lead to enhanced humoral and cellular (Th1 and/or CTL) immune responses (Singh et al., 2000; Kazzaz et al., 2000; Cui and Mumper, 2002a; Cui and Mumper 2002b; Kreuter and Speiser, 1976).

There have been several reports that chemically modifying a protein antigen to make it more positively-charged (a process termed 'cationization') sufficiently enhanced its immunological properties without changing the antigens' specificity (Pardridge et al., 1994a,b; Muckerheide et al., 1987). For example, Muckerheide et al. (1987) demonstrated that native bovine serum albumin (nBSA) and cationized BSA (cBSA) can cross react at the B cell level as evidenced by both the ability of the antibody raised against one form to react with the other, and by inhibition assays using ELISA. Moreover, 500-times less cBSA was required to elicit the same level of immune response as compared with nBSA. The immune response elicited with the cBSA peaked later and lasted longer than that elicited by the nBSA. Moreover, antibodies were produced in response to administration of cBSA, but not nBSA, when injected intravenously without any adjuvant.

The overall goal of this work was to cationize a model protein antigen, β-galactosidase, coat the cationized protein on the surface of novel anionic nanoparticles engineered from microemulsion precursors, and assess the immune response of this system after subcutaneous injection to mice. It was our hypothesis that the combined system would result in enhanced humoral and cellular (Th1-type) immune responses after subcutaneous injection in mice.

2. Materials and methods

2.1. Materials

Emulsifying wax and β-galactosidase were purchased from Spectrum Quality Products, Inc. (New Brunswick, NJ). Sodium dodecyl sulfate (SDS), 1-ethyl-3-(3-dimethylaminopropyl)-carbodiimide Hydrochloride (EDC), Hexamethylenediamine (HMD), basic fuchsin, glycine, normal goat serum (NGS), and Sephadex G-75 were from Sigma Chemical Co. (St. Louis, MO). PBS/Tween

20 buffer (20X) was obtained from Scyteck Laboratories (Logan, UT). Tetramethylbenzidine (TMB) Substrate Kit was from Pierce (Rockford, IL). Anti-mouse IgG peroxidase-linked species specific $F(ab')_2$ fragment (from sheep) was purchased from Amersham Pharmacia Biotech Inc. (Piscataway, NJ). Mouse Interleukin-2 (IL-2), IL-4, and Interferon-γ (IFN-γ) ELISA Kits were purchased from Endogen, Inc. (Woburn, MA).

2.2. Methods

2.2.1. Engineering of anionic nanoparticles from microemulsion precursors

Emulsifying wax (2 mg) was accurately weighed into 7-ml glass scintillation vials and melted on a hot plate at 50–55 °C. Required volumes of deionized and filtered (0.22 μm) water were added to the melted wax while stirring to form homogenous milky slurries. Various volumes of a SDS stock solution (50 mM) were added while stirring to obtain final SDS concentrations from 1 mM to 30 mM. Within seconds, clear O/W microemulsions formed, if the final SDS concentration was within an appropriate range. The droplet size of the microemulsion was measured at 55 °C using a Coulter N4 Plus Sub-Micron Particle Sizer (Coulter Corporation, Miami, FL) at 90° light scattering for 90 s. These microemulsions were then simply cooled (cured) to room temperature while stirring to form nanoparticles. For particle sizing, the nanoparticle suspension was diluted with deionized and filtered (0.22 μm) water and the particle size was measured at 90° light scattering for 90 s at 25 °C. The zeta potentials of engineered nanoparticles were also measured using a Zeta Sizer 2000 from Malvern Instruments, Inc. (Southborough, MA).

2.2.2. Stability of engineered anionic nanoparticles in aqueous suspension

Cured nanoparticle suspensions as described in Section 2.2.1 were sealed, and stored at room temperature over 6 days. In order to investigate the effect of dilution on the stability of the cured nanoparticles, the same nanoparticle suspension was diluted 10-fold with deionized and filtered (0.22 μm) water, sealed and stored as above. The particle size was measured each day for 6 days. Within 5 min prior to particle sizing, the nanoparticle suspension was diluted with water, if necessary, to maintain the total light scattering intensity (in counts per second, cps) in the required range of the N4 Plus Sub-Micron Particle Sizer (5×10^4 to 1×10^6 cps).

2.2.3. Stability of engineered anionic nanoparticles in isotonic solutions

In order to investigate the stability of the nanoparticles in simulated biological media and to identify a suitable vehicle for injection, cured nanoparticle suspensions were also diluted 10-fold with either 10% lactose, 10 mM phosphate buffered saline (pH 7.4), 150 mM NaCl (normal saline), or 10% (v/v) FBS in saline, and the particle size was measured over 30 min at 37 °C. For the 10% (v/v) FBS challenge, the stability of GPC-purified nanoparticles was also investigated.

2.2.4. Purification of engineered anionic nanoparticles

To separate free SDS from the nanoparticles, gel permeation chromatography (GPC) using Sephadex G-75 was performed. Sephadex G-75 was pre-soaked with de-ionized and filtered (0.22 μm) water overnight and then packed in a 15×70 mm plastic column. The column was equilibrated with 10% w/v lactose. Three hundred microliters (300 μl) of the cured nanoparticle suspension was applied to the column, and the eluent was collected in 1 ml fractions in plastic vials. The collected fractions were then analyzed by laser light scattering using the N4 Plus Sub-Micron Particle Sizer to identify the fraction containing nanoparticles and SDS. In all cases, the fourth fraction contained the greatest number of nanoparticles, as evidenced by laser light scattering and zeta potential measurements. The effectiveness of the GPC purification was verified by passing 300 μl of free SDS solution (same concentration used in the nanoparticle preparation) through the same GPC column. The concentration of the SDS in every eluent fraction was measured to make sure the majority of the free SDS did not elude in fraction 4. The free SDS concentration in each fraction was quantified using the basic fuchsin spectropho-

tometric method (Waite et al., 1976). Briefly, a standard curve was constructed by making a series of SDS solutions (1 ml) with concentration ranging from 0 to 100 mM in glass tubes. One milliliter each of 0.03 M HCl, and 48 mg/l basic fuchsin, and 2 ml of chloroform were added to each tube. The tubes were mixed, vortexed briefly, and heated at 60 °C for 15 min. After removing off the upper aqueous phase, the lower phase of SDS-fuchsin in chloroform was read at 553 nm in a U-2000 Hitachi spectrophotometer. The GPC eluent samples were treated similarly, and the SDS concentration in each fraction was converted from the standard curve.

2.2.5. Cationization of β-galactosidase

β-galactosidase was cationized as previously described with some modification (Pardridge et al., 1994a,b Muckerheide et al., 1987). Briefly, 20 mg of β-galactosidase (Spectrum) was dissolved into 1 ml of PBS buffer (10 mM, pH 7.4). Then, 2 ml of HMD (2 M, pH 6.8) and 54 mg of EDC were added into the protein solution. After the pH was adjusted to 6.8 with concentrated HCl, the mixture was stirred at room temperature for 3 h. The reaction was stopped by adding 1 ml of glycine solution (2 M) and stirred for another 1 h. Cationized proteins were purified with a Sephadex G-25 column (Prepacked PD-10, Amersham Pharmacia) and concentrated with ultra-centrifugation filter tubes (100 kDa cut-off) from Eppendorf Scientific, Inc. (Westbury, NY). Protein concentration was determined using the Coomassie® Plus Protein Assay Reagent (Pierce). Verification of cationization was completed by electrophoresis on 1% Seakem® Gold agarose gel (FMC BioProducts, Rockland, ME) in Tris-Acetate-EDTA buffer (TAE, pH 7.4) (Sigma). Gel was stained with the Coomassie® Plus for 30 min to visualize the position of the proteins.

2.2.6. Surface coating of cGal on anionic nanoparticles

Cationized β-galactosidase (cGal) was coated on the surface of the GPC purified anionic nanoparticles by gently mixing the required amount of cGal with 1 ml of purified nanoparticles in suspension to obtain a final cGal concentration of 100 μg/ml. At least 30 min at room temperature was allowed for complete adsorption of cGal to the surface of the nanoparticles before particle sizing and TEM were performed.

2.2.7. Transmission electron micrographs (TEM)

The size and morphology of nanoparticles were observed using TEM (Philips Tecnai 12 Transmission Electron Microscope) in the Electron Microscopy & Imaging Facility at the University of Kentucky Medical Center. A carbon coated 200-mesh copper specimen grid (Ted Pella, Inc., Redding, CA) was glow-discharged for 1.5 min. Nanoparticle suspension deposition on the grid and uranyl acetate staining was completed as previously described (MacLaughlin et al., 1998).

2.2.8. Mouse immunization studies

Ten to twelve week old female mice (Balb/C) from Harlan Sprague-Dawley Laboratories were used for all animal studies. NIH guidelines for the care and use of laboratory animals were observed. Mice ($n = 4–5$/group) were immunized by subcutaneous injection on days 0, 7, and day 14 with either nGal (10 μg) adjuvanted with 'Alum' (15 μg), cGal (10 μg) alone, or cGal (10 μg) coated on anionic nanoparticles. Prior to immunization, mice were anesthetized using pentobarbital (i.p.). One hundred microliters of each formulation in 10% lactose was injected on one site on the back. On day 28, the mice were anesthetized and bled by cardiac puncture. Sera were separated and stored as previously described (Cui and Mumper, 2001a). β-galactosidase-specific serum IgG titer were quantified by ELISA (Cui and Mumper, 2001a). Spleens from all naïve and immunized mice were also removed, pooled for each group, and processed as previously described (Cui and Mumper, 2001b). Cytokine release assays from stimulated splenoctyes were performed as previously described (Cui and Mumper, 2001b). Briefly, isolated splenocytes (5×10^6/well) with three replicates were stimulated with β-galactosidase protein (3.3 μg/well) for 60 h at 37 °C. Cytokine release was quantified using ELISA kits from Endogen. Statistical analysis was completed using a two-sample t-test assuming unequal variances. A P-value < 0.05 was considered to be statistically significant.

3. Results and discussion

3.1. Engineering of anionic nanoparticles from microemulsion precursors

Anionic nanoparticles were engineered directly from oil-in-water (O/W) microemulsion precursors in a single vessel, one-step process. When the required volume of SDS (50 mM) was added into the homogenous milky slurry of melted emulsifying wax in water at 50–55 °C, the suspension turned clear within seconds if the final SDS concentration was ≥ 10 mM. For samples having a final SDS concentration of < 10 mM, the turbidity of the samples decreased but did not turn clear even after prolonged stirring at 55 °C. For all samples, the microemulsion droplet sizes at 55 °C were in the range of 45–70 nm as shown in Table 1. Systems made without SDS were not sized since O/W microemulsions were not formed and the emulsifying wax precipitates were greater than the upper limit of the PCS instrument (i.e., 3 microns). By simple cooling of the O/W microemulsions to room temperature while stirring, anionic nanoparticles were formed with diameters around 100 nm when the final SDS concentration was ≥ 10 mM. For reasons not yet understood, the diameters of cured anionic nanoparticles were 22–48% larger than the corresponding microemulsion droplet size. This effect may be real or an artifact due to the difference in light scattering of liquid droplets at 55 °C and solid nanoparticles at 25 °C. Nevertheless, this effect is consistently observed by our laboratory for a number of different types of O/W microemulsion precursors used to engineer solid nanoparticles (Cui and Mumper, 2001b; Cui and Mumper 2002a,b; Oyewumi and Mumper, 2002). As expected, the zeta potential of the nanoparticles engineered with SDS, a negatively-charged surfactant, were negative using all SDS concentrations. As the final SDS concentration increased from 10 to 25 mM the zeta potential of the nanoparticles remained unchanged since there was no statistical difference between the zeta potentials of nanoparticles made with a final SDS concentration between 10 and 25 mM ($P = 0.07$ between all groups; ANOVA). The zeta potential of nanoparticles made with a final SDS concentration of 30 mM of -67 mV was statistically different from that of nanoparticles made with final SDS concentrations between 10 and 25 mM ($P < 0.05$; ANOVA). It is speculated that the more negative zeta potential of nanoparticles made with 30 mM SDS was due to the presence of SDS micelles. As the number of the micelles increased, the viscosity of the medium that the nanoparticles are dispersed in will increase (Martin et al., 1983). Since the viscosity of the medium

Table 1
The physical properties of anionic nanoparticles engineered from microemulsion precursors using sodium dodecyl sulfate (SDS) as an anionic surfactant

Final [SDS] (mM)	Microemulsion size (nm)	Nanoparticle size (nm)	Zeta potential (mV)
1	N/A	425 ± 184 (0.724)	−84 ± 1
5	N/A	298 ± 116 (0.386)	−73 ± 6
10	59 ± 19 (0.185)	96 ± 36 (0.296)	−62 ± 2[a]
15	48 ± 17 (0.247)	90 ± 25 (0.117)	−49 ± 6[a]
20	50 ± 19 (0.322)	99 ± 22 (0.061)	−61 ± 4[a]
25	52 ± 21 (0.348)	97 ± 35 (0.275)	−60 ± 4[a]
30	70 ± 18 (0.084)	113 ± 46 (0.503)	−67 ± 2[b]

The microemulsion droplet size at 55 °C and the cured nanoparticle size at 25 °C and zeta potential are shown as a function of the final SDS concentration. Microemulsion precursors (1 ml) were prepared at 55 °C with emulsifying wax (2 mg/ml) in water using SDS (1–30 mM) as the surfactant. Nanoparticles were engineered by simple cooling of the microemulsion precursor to room temperature. The data reported for microemulsion droplet size, and nanoparticle size are mean ± S.D. (polydispersity index); the zeta potential data are the mean ± S.D. ($n = 3$).

[a] Indicates that the results are statistically the same for all values ($P = 0.07$; ANOVA).

[b] Indicates that the results are statistically different for all values marked by superscript a ($P < 0.05$; ANOVA).

is proportional to the zeta potential of the nanoparticles dispersed in, it is reasonable to observe that the nanoparticles become more negative as the concentration of the SDS increases (Martin et al., 1983). For reasons not yet understood, precipitates made with final SDS concentration ≤ 5 mM resulted in systems having zeta potentials that were quite negative (-73 mV and -84 mV). It is possible that this phenomenon may be caused, in part, by the formation of larger precipitates when using lower concentrations of final SDS. Again, with less SDS, less amount of the emulsifying wax will be in microemulsion, leading to the increase in the viscosity of the disperse medium. Nevertheless, this underscored the necessity for having a minimum effective concentration of SDS (i.e., 10–15 mM) present in the system to form a stable O/W microemulsion precursor. As illustrated in Table 1, solid nanoparticles having diameters $<$ 100 nm could not be engineered unless the final SDS concentration was ≥ 10 mM.

3.2. Stability of engineered anionic nanoparticles in aqueous suspension

A short-term nanoparticle stability study was completed to identify the most appropriate final SDS concentration used to engineer stable nanoparticles. In this study, the effect of dilution on the stability of the nanoparticles in suspension was also investigated. As shown in Fig. 1, undiluted nanoparticles in suspension were more stable than diluted nanoparticles over the six day storage period when the final SDS concentration was ≥ 10 mM. Although short-term stability study showed that anionic nanoparticles prepared with 15 mM of SDS had the greatest stability, the size of these nanoparticles still increased by $\sim 57\%$ over 6 days stored at room temperature under undiluted condition. Additional insight is still needed to fully optimize the stability of the engineered nanoparticles over time. We are currently assessing optimal storage conditions of these nanoparticles over time including optimal storage conditions after lyophilization. Based on the results above, the nanoparticles engineered with a final SDS concentration of 15 mM were selected for further study based on the small size of the cured nanoparticles (78 ± 11 nm), the relatively low final SDS concentration, and the relative stability of the cured nanoparticles over time.

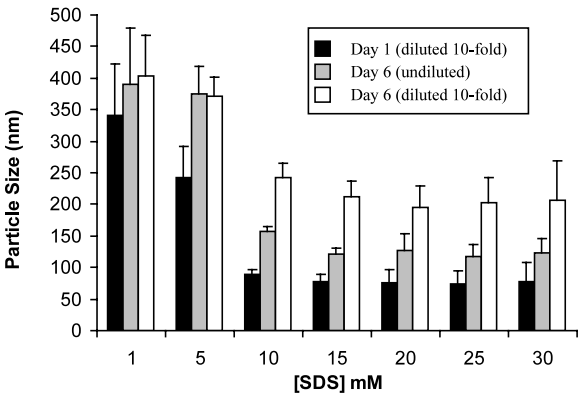

Fig. 1. The stability of engineered anionic nanoparticles in aqueous suspension. A short-term stability of the cured nanoparticles (from Table 1) in aqueous suspension and the effect of dilution on this stability were investigated by measuring the size of the cured nanoparticles, diluted 10-fold with water or undiluted, at room temperature over 6 days. The data reported are the mean $\pm$ S.D. ($n = 3$).

3.3. Stability of engineered cationic nanoparticles in isotonic solutions

In order to identify a suitable vehicle for injection, the stability of the anionic nanoparticles in different isotonic solutions was measured at 37 °C over 30 min. As shown in Fig. 2, there was no significant change in particle size of the nanoparticles in 10% lactose, 10 mM phosphate buffered saline (pH 7.4), or 150 mM NaCl at 37 °C over 30 min. Unpurified anionic nanoparticles in the FBS/saline (10%, v/v) mixture tended to aggregate. For example, when sized just immediately after addition of FBS/saline, the nanoparticles were 332 ± 151 nm with a polydispersity index of 1.226 (Fig. 2). However, after GPC purification with Sephadex G-75 as described below, the nanoparticles were found to be stable at 37 °C over 30 min (from 123 ± 51 nm to 147 ± 60 nm), providing evidence that free SDS is at least partially related to the aggregation.

3.4. Purification of engineered cationic nanoparticles

The observation that unpurified nanoparticles aggregated in the FBS/Saline (10:90 v/v) prompted investigation into methods to purify the engineered nanoparticles to remove free SDS. In addition to causing instability, free SDS in the nanoparticle preparations may interfere with the coating of nanoparticles with cationized protein by the formation of a SDS/protein complex or micelle aggregates. Thus, SDS was removed by GPC (Sephadex G-75) using 10% lactose as the mobile phase. As confirmed in Fig. 3, free SDS could easily be removed from the anionic nanoparticles using GPC. As expected, nanoparticles eluded in the void volume or fraction 4, while the majority of the free SDS eluded out in the GPC-fractionated volumes (fractions 10–15).

Again, it is important to note that the basic fuchsin assay for SDS can only detect free SDS, not SDS either coated on the surface of, or embedded in, the nanoparticles. Using mass balance analysis, it was estimated that about 1/3 of the total SDS used to engineer the nanoparticles was associated with nanoparticles. It was also observed that the GPC purification process had no effect on the size of the anionic nanoparticles (data not shown).

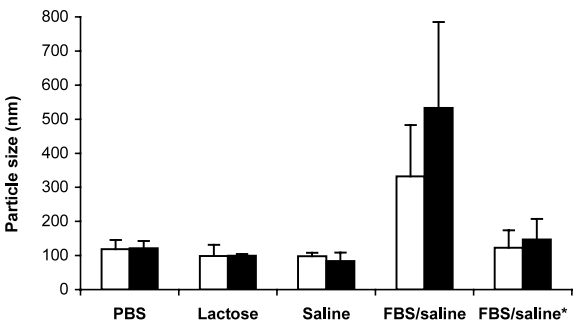

Fig. 2. The stability of the anionic nanoparticles in various isotonic vehicles at 37 °C over 30 min. For particle size measurements, 100 μl of each sample was diluted with 900 μl 10 mM phosphate buffered saline, pH 7.4 (PBS), 10% lactose (Lactose), 150 mM NaCl (saline), or 10% (v/v) FBS in saline. The nanoparticles were engineered from microemulsion precursors comprised of emulsifying wax (2 mg) and SDS (15 mM) in 1 ml water. White bars, nanoparticle size at 0 min; black bars, nanoparticle size at 30 min. FBS/saline* is the stability of the GPC-purified anionic nanoparticles in 10% (v/v) FBS in saline.

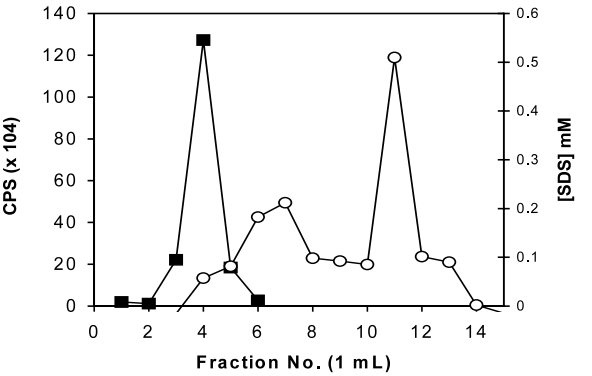

Fig. 3. Gel permeation chromatography (GPC) purification of the anionic nanoparticles. Free SDS was separated from the nanoparticles using a 15 × 70 mm Sephadex G75 column. The column was equilibrated with 10% w/v lactose. Three hundred microliters (300 μl) of the cured nanoparticle suspension was applied to the column; and the eluent was collected in 1 ml fractions. The collected fractions were then analyzed by laser light scattering using the N4 Plus Sub-Micron Particle Sizer to identify the fraction containing nanoparticles as evidenced by light scattering in counts per second (cps ■). The SDS concentration (○) in each fraction was quantified using basic fuchsin spectrophotometric method. The effectiveness of the GPC purification was verified by passing 300 μl of free SDS solution (same concentration as used in the nanoparticle preparation) through the same GPC column. The concentration of SDS in each fraction was measured to verify that the majority of the free SDS did not elude in fraction 4 (data not shown).

3.5. Cationization of β-galactosidase

Cationization of protein antigens has been reported by a few groups to alter the immunological properties of the protein without changing the antigen's specificity (Pardridge et al., 1994a,b; Muckerheide et al., 1987). β-galactosidase protein (nGal) was cationized for coating on the surface of the anionic nanoparticles, and at the same time, to further investigate the effect of cationization on the immunological properties of a protein antigen. The pI of β-galactosidase (nGal) was reported to be 4.6 (Wallenfels and Weil, 1972). The nGal moved toward the cathode as shown in Fig. 4. However, cationized β-galactosidase (cGal)

moved toward the anode confirming that the pI of the cGal was greater than 7.4 since the TAE buffer used in the gel electrophoresis method had a pH of 7.4. Attempts were not made to determine the actual pI of the cGal protein.

3.6. Coating of cGal on anionic nanoparticles and TEM

Cationized β-galactosidase (cGal) was coated on the surface of the GPC purified anionic nanoparticles by gently mixing the required amount of cGal with 1 ml of GPC purified nanoparticles in 10% lactose to obtain a final cGal concentration of 100 μg/ml. Care was taken to find appropriate amount of both cGal and anionic nanoparticles to avoid aggregation. It was observed that the coating of cGal increased the viscosity of the nanoparticle suspension (data not shown). The size of the cGal-coated nanoparticles, obtained by laser light scattering using PCS ranged from 208 to 354 nm. Fig. 5 shows the TEM micrographs of the unpurified anionic nanoparticles (Fig. 5A) and purified nanoparticles coated with cGal (Fig. 5B). As expected, both unpurified anionic nanoparticles and cGal-coated nanoparticles were spherical or close to spherical. The particle sizes as determined by the TEM micrograph for the uncoated anionic nanoparticles were in general agreement with those sizes measured by PCS ($\sim$ 100 nm). However, the sizes of the cGal-coated GPC-purified nanoparticles measured by TEM micrograph appeared smaller than those sizes as measured by PCS (Fig. 5B). The reason for this is not clear, but may be due to slight increases in viscosity of the cGal-coated nanoparticle systems that were not corrected for when sizing using PCS. Alternatively, differences in particles sizes between TEM and PCS may be explained by the fact that the TEM method involves the dehydration of nanoparticles to coat the carbon coated copper grid, whereas the PCS method involves the scattering of light by nanoparticles in aqueous suspension. Nevertheless, the TEM micrographs demonstrate that the surface morphology of the nanoparticles was changed after coating with cGal, as evidenced by the unique darker staining pattern at the edge of the nanoparticles (Fig. 5B). In addition, the surface of the protein-coated nanoparticles is not as sharp as that of the uncoated nanoparticles and the protein-coated nanoparticles appear to be less spherical (Fig. 5B).

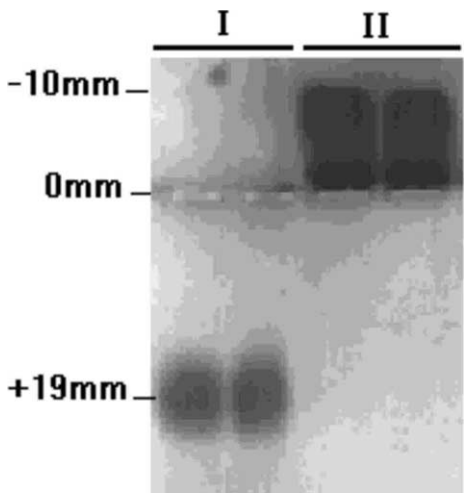

Fig. 4. Verification of the cationization of β-galactosidase by agarose gel electrophoresis. β-galactosidase was cationized as mentioned in Section 2. Verification of cationization was completed by electrophoresis on 1% Seakem® Gold agarose gel in Tris-Acetate-EDTA buffer (TAE, pH 7.4). Gel was stained using Coomassie® Plus for 30 min to visualize the position of the proteins. I corresponds to native β-galactosidase protein (nGal); II corresponds to cationized β-galactosidase protein (cGal). 0 mm indicates the well position on the gel. + 19 indicates the nGal ran toward the cathode for 19 mm, while − 10 mm indicates that the cGal run towards the anode for 10 mm.

3.7. Immune responses in mice

Fig. 6 shows the β-galactosidase-specific total IgG titer in mouse sera 28 days after subcutaneously injection of nGal adjuvanted with 'Alum', cGal alone (without adjuvant), or cGal-coated anionic nanoparticles. Cationized β-galactosidase (cGal) alone elicited similar humoral immune responses to nGal adjuvanted with 'Alum' ($P = 0.37$). These results in general agree with other reports using cationized protein antigens wherein native protein antigen and cationized protein antigen can cross react at the B cell level as evidenced by the ability of the antibody raised against

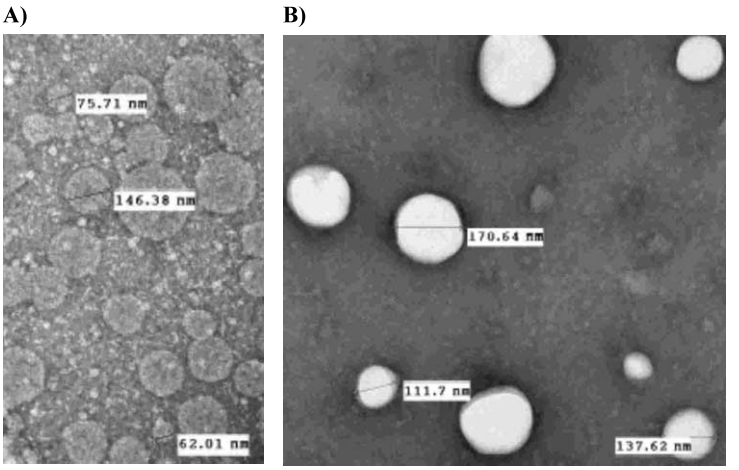

Fig. 5. Transmission electron micrograph (TEM) of the nanoparticles. (A) TEM of unpurified anionic nanoparticles. The nanoparticles were prepared with emulsifying wax (2 mg/ml) and SDS (15 mM) as in Table 1. (B) TEM of GPC purified, cGal-coated nanoparticles. The nanoparticles in Fig. 5A were purified by GPC, and the required amount of cGal was coated on their surface to obtain a final cGal concentration of 100 μg/ml.

cationized protein antigen to recognize the native antigen (Pardridge et al., 1994a,b Muckerheide et al., 1987). In contrast, coating of cGal on the surface of anionic nanoparticles resulted in significantly enhanced antigen-specific IgG titer over both the nGal with 'Alum' ($P = 0.03$) and cGal alone ($P = 0.008$). Also, mice immunized with cGal-coated nanoparticles resulted in very reproducible responses with all mice in the group having equal IgG titer.

In Table 2, the cytokine release data from isolated splenocytes after in-vitro stimulation with β-galactosidase is shown. As expected, immunization with nGal with 'Alum' produced relatively low levels of Th1 cytokines. In contrast, the splenocytes from mice immunized with cGal alone produced very high levels of Th1 cytokines that were significantly enhanced over both cGal-coated nanoparticles and nGal. For example, splenocytes from mice immunized with cGal alone produced IL-2 and IFN-γ that were 18-fold and 8-fold greater, respectively, than splenocytes from mice immunized with nGal with 'Alum'. The IL-4 level from splenocytes isolated from mice immunized with the cGal-coated nanoparticles was 3–4-fold greater than that from the nGal or cGal immunized mice, strongly suggesting an enhanced Th2-

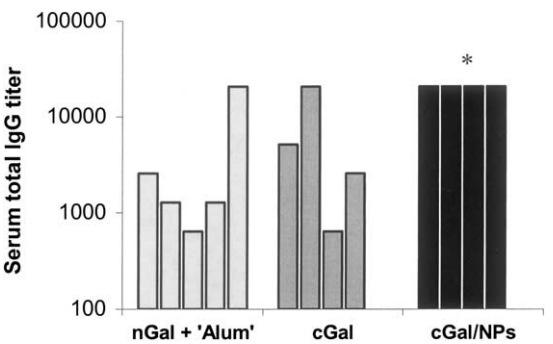

Fig. 6. Antigen-specific total IgG titer in serum to β-galactosidase 28 days after subcutaneous administration. One hundred microliters (100 μl) of the formulations containing 10 μg of β-galactosidase were injected in anesthetized Balb/C mice $n = 4–5$ on day 0, day 7, and day 14. The groups were: (white bars) nGal, 10 μg of β-galactosidase protein adjuvanted with 15 μg 'Alum'; (gray bars) cGal, 10 μg of cationized β-galactosidase protein; (black bars) cGal/NSp, 10 μg of cationized β-galactosidase protein coated on the surface of GPC purified, sterile-filtered anionic nanoparticles. * indicates that the mean IgG titer of cGal/NSp was significantly different from that of the nGal and cGal. Statistical analysis was completed using a two-sample t-test assuming unequal variances. A result of $P < 0.05$ was considered statistically significant.

Table 2
In-vitro cytokine release from isolated splenocytes after stimulation with β-galactosidase for 60 h

	Th1 type		Th2 type
	IL-2 (pg/ml)	IL-4 (pg/ml)	IFN-γ (pg/ml)
Naïve	545 ± 54	460 ± 30	Undetectable
nGal	171 ± 13	$4{,}340 \pm 170$	164 ± 15
cGal	3184 ± 83[a]	$32{,}690 \pm 5900$[a]	121 ± 16
CGal/NPs	2288 ± 298[b]	$10{,}520 \pm 3600$[b]	408 ± 24[c]

Mice were immunized with 10 μg β-galactosidase on day 0, 7, and 14 by subcutaneous injection. On day 28, the spleens were removed and pooled for each group. Isolated splenocytes (5×10^6/well) with three replicates were stimulated with β-galactosidase protein (3.3 μg/well) for 60 h at 37 °C. Cytokine release was quantified using ELISA kits (Endogen). Groups are the same as in Fig. 6: nGal, 10 μg of β-galactosidase protein adjuvanted with 15 μg 'Alum'; cGal, 10 μg of cationized β-galactosidase protein; cGal/NPs, 10 μg of β-galactosidase protein coated on the surface of GPC purified, sterile-filtered anionic nanoparticles.

[a] Indicates that the results for cGal were significantly different from that of both nGal and cGal/NPs.

[b] Indicates that the results for cGal/NPs were significantly different from that of both nGal and cGal.

[c] indicates that the results for (IFN-gamma) cGal/NPs were significantly different from that of both nGal and cGal. The reported data are the mean + S.D. Statistical analysis was completed using a two-sample t-test assuming unequal variances. A result of $P < 0.05$ was considered statistically significant.

type immune response. Interestingly, cGal-coated nanoparticles also enhanced the Th1-type cytokine release (IL-2 and IFN-γ), compared to mice immunized with nGal with 'Alum'. A more balanced enhancement of both Th1-type and Th2-type immune responses as observed with the cGal-coated nanoparticles was somewhat surprising since it is generally understood that vaccination methods that promote strong Th2-type immune responses (high antibody and strong Th2-type cytokines) tend to produce weak Th1-type immune responses, and vice-versa (Abbas et al., 1996; Seder and Paul, 1994). Additional studies are going on to better elucidate possible mechanisms of immune response with cGal-coated nanoparticles.

We reported previously that cationic and neutral nanoparticles having diameters below 100 nm could be generated from oil-in-water (O/W) microemulsion using emulsifying wax as the oil phase and either CTAB or Brij 78 as cationic or neutral surfactant (Cui and Mumper, 2001b, 2002a,b; Oyewumi and Mumper, 2002). Emulsifying wax (anionic) is comprised of cetyl alcohol and polysorbate 60 in a molar ratio of about 20:1. The wax was typically used in cosmetics and topical pharmaceutical formulations. For example, cetyl alcohol is an excipient in the marketed product Exosurf Neonatal® and polysorbate 60 is used in many pharmaceutical formulations including parenterals. Previous studies using the cationic (CTAB) nanoparticles coated with pDNA, no gross inflammatory, allergic, and toxic effects have been observed in mice after subcutaneous, intramuscular, and topical administration (Cui and Mumper, 2001b, 2002a,b). The nanoparticles in the present study were prepared with SDS as an anionic surfactant. SDS is typically used as an anti-bacterial agent in formulations like capsules and tablets (Wade et al., 1994). Although the toxicity of SDS needs further investigation, subcutaneous administration of these SDS nanoparticles did not cause any gross adverse effects.

The process to engineer nanoparticles via the O/W microemulsion precursors has several advantages as follows: (i) the process involves only one step in one vessel; (ii) the process is rapid, reproducible and is readily scalable; (iii) the process does not require the use of expensive and damaging high-torque mechanical mixing, microfluidization, or homogenization. Ideally, these engineered nanoparticles are quite versatile as we have previously demonstrated that various types of agents such as endosomolytic lipids and cell-targeting ligands can be included in these systems (Cui and Mumper, 2001b). It is believed that these engineered nanoparticles may have potential utility against pathogens that require both enhanced humoral and cellular-based immune responses.

References

Abbas, A.K., Murphy, K.M., Sher, A., 1996. Functional diversity of helper T lymphocytes. Nature 383, 787–793.

Alving, C.R., 1991. Liposomes as carrier of antigens and adjuvants. J. Immunol. Methods 140, 1–13.

Cui, Z.R., Mumper, R.J., 2001a. Chitosan-based nanoparticles for topical genetic immunization. J. Control. Rel. 75, 409–419.

Cui, Z.R., Mumper, R.J., 2001b. Dendritic cell-targeted genetic vaccines engineered from novel microemulsion precursors. Mol. Ther. 3, S352.

Cui, Z.R., Mumper, R.J., 2002a. Enhanced humoral and proliferative immune responses after topical application of nanoengineered genetic vaccine, J. Control. Rel. in press.

Cui, Z.R., Mumper, R.J., 2002b. Genetic immunization using nanoparticles engineered from microemulsion precursors, Pharm. in press.

Gupta, R.K., Relyveld, E.H., Lindblad, E.B., et al., 1993. Adjuvants—a balance between toxicity and adjuvanticity. Vaccine 10, 96–97.

Gupta, R.K., Siber, G.R., 1995. Adjuvants for human vaccines—current status, problems and future prospects. Vaccine 13, 1263–1276.

Kazzaz, J., Neidleman, J., Singh, M., Ott, G., O'Hagan, D.T., 2000. Novel anionic microparticles are a potent adjuvant for the induction of cytotoxic T lymphocytes against recombinant p55 gag from HIV-1. J. Control. Rel. 67, 347–356.

Kensil, C.R., 1996. Saponins as vaccine adjuvants. Crit. Rev. Ther. Drug Carrier Syst. 13, 1–55.

Kreuter, J., Speiser, P.P., 1976. New adjuvants on a poly(-methylacrylate) base. Infect. Immun. 13, 204–210.

MacLaughlin, F.C., Mumper, R.J., Wang, J., Tagliaferri, J., Gill, I., Hinchcliffe, M., Rolland, A.P., 1998. Chitosan and depolymerized chitosan oligomers as condensing carriers for in vivo plasmid delivery. J. Control. Rel. 56, 259–272.

Martin, A., Swarbrick, J., Cammarata, A., 1983. Physical Pharmacy: Physical Chemical Principles in the Pharmaceutical Sciences, 3rd ed. Lea & Febiger, Philadelphia, PA.

Morein, B., Fossum, C., Lovgren, K., Hoglund, S., 1990. The ISCOMS—a modern approach to vaccines. Semin. Virol. 1, 49–55.

Moser, C.A., Speaker, T.J., Offit, P.A., 1997. Effect of microencapsulation on immuno-genicity of a bovine herpes virus glycoprotein and inactivated influenza virus in mice. Vaccine 15, 1767–1772.

Muckerheide, A., Apple, R.J., et al., 1987. Cationization of protein antigens I. Alteration of immunogenic properties. J. Immunol. 138, 833–837.

Muller, R.H., Mader, K., Gohla, S., 2000. Solid lipid nanoparticles for controlled drug delivery—a review of the state of the art. Eur. J. Pharm. Biopharm. 50, 161–177.

Ocampo, V., Salazar, J.E., et al., 2000. Clinical and humoral immune responses of cattle vaccinated with an experimental inactivated Anaplasma marginale vaccine in 2 different adjuvants. 3rd Ann. Conf. Vaccine Res. Washington DC, USA 30 April–2 May.

O'Hagan, D.T., 1997. Recent advances in vaccine adjuvants for systemic and mucosal administration. J. Pharm. Pharmacol. 49, 1–10.

O'Hagan, D.T., Rahman, D., et al., 1991. Biodegradable microparticles as controlled release antigen delivery systems. Immunology 73, 239–242.

Oyewumi, M.O., Mumper, R.J. 2002. Gadolinium loaded nanoparticles engineered from microemulsion templates. Drug. Dev. Ind. Pharm. in press.

Pardridge, W.M., Bickel, U., Buciak, J., Yang, J., Diagne, A., 1994a. Enhanced endocytosis and anti-human immunodeficiency virus type 1 activity of anit-rev antibodies after cationization. J. Infect. Dis. 169, 55–61.

Pardridge, W.M., Bickel, U., Buciak, J., Yang, J., Diagne, A., Aepinus, C., 1994b. Cationization of a monoclonal antibody to the human immunodeficiency virus REV protein enhances cellular uptake but does not impair antigen binding of the antibody. Immunol. Lett. 42, 191–195.

Plotkin, S.L., Plotkin, S.A., 1988. A short history of vaccination. In: Plotkin, S.A., Mortimer, E.A. Jr. (Eds.), Vaccine, 2nd ed. W.B. Saunders Company, Philadelphia, pp. 1–11.

Seder, R.A., Paul, W.E., 1994. Acquisition of lymphokine producing phenotype by CD4+ T cells. Annu. Rev. Immunol. 12, 635–673.

Sheikh, N.A., Al-Shamisi, M., Morrow, W.J.W., 2000. Delivery systems for molecular vaccination. Curr. Opinion Mol. Therapeut. 2, 37–54.

Singh, M., Briones, M., Ott, G., O'Hagan, D.T., 2000. Cationic microparticles: a potent delivery system for DNA vaccines. Proc. Natl. Acad. Sci. USA 97, 811–816.

Singh, M., O'Hagan, D., 1999. Advances in vaccine adjuvants. Nat. Biotech. 17, 1075–1081.

Wade, A., Weller, P.J. (Eds.), 1994. Handbook of Pharmaceutical Excipients, 2nd ed. The Pharmaceutical Press, London, England and the American Pharmaceutical Association, Washington, DC.

Waite, J.H., Wang, C.Y., 1976. Spectrophotometric measurement of sodium dodecyl sulfate with basic fuchsin. Anal. Biochem. 70, 279–280.

Wallenfels, K., Weil, R., 1972. Beta-Galactosidase. In: Boyer, P.D. (Ed.), The Enzymes, vol. 7, third ed. Academic Press, New York, pp. 617–663.